Strain Rate Effects on the Energy Absorption of Rapidly Manufactured Composite Tubes

Aaron Brighton, Mark Forrest, Mike Starbuck, Donald Erdman and Bronwyn Fox

Journal of Composite Materials 2009 43: 2183 originally published online 5 August 2009
DOI: 10.1177/0021998309344646

Strain Rate Effects on the Energy Absorption of Rapidly Manufactured Composite Tubes

AARON BRIGHTON,[1,*] MARK FORREST,[1] MIKE STARBUCK,[2]
DONALD ERDMAN[2] AND BRONWYN FOX[1]
[1]*Institute for Technology Research and Innovation, Deakin University Geelong, VIC, Australia*
[2]*Oak Ridge National Laboratory, Tennessee, USA*

ABSTRACT: Quasi-static and intermediate rate axial crush tests were conducted on tubular specimens of Carbon/Epoxy (Toray T700/G83C) and Glass/Polypropylene (Twintex). The quasi-static tests were conducted at 10 mm/min (1.67×10^{-4} m/s); five different crush initiators were used. Tests at intermediate rates were performed at speeds of 0.25, 0.5, 0.75, 1, 2, and 4 m/s. Modes of failure and specific energy absorption (SEA) values were studied. The highest SEA measured was 86 kJ/kg. This value was observed using Carbon/Epoxy samples at quasi static rates with a 45° chamfer initiator. The highest energy absorption for Twintex tubes was observed to be 57.56 kJ/kg during 45° chamfer initiated tests at 0.25 m/s. Compared with steel and aluminium, SEA values of 15 and 30 kJ/kg, respectively, the benefits of using composite materials in crash structures become apparent.

KEY WORDS: carbon fibre, glass fibre, energy absorption, mechanical testing.

INTRODUCTION

AS DISCUSSED BY Dreyfus and Viscusi [1] automotive safety has long been regulated and mandated by government and with the introduction of corporate average fuel economy standards and European Union directives regarding emissions, automotive manufactures are looking for new ways to meet these regulations [2].

If modern lightweight materials are used in crash structures then vehicle fuel economy can be improved. Increasing and improving the manner in which energy is absorbed within the crush zones in automotive vehicles can also substantially improve vehicle safety. As a result of their excellent crash characteristics and high strength to weight ratios, carbon fibre composites offer a solution to fulfill both of these requirements simultaneously.

*Author to whom correspondence should be addressed. E-mail: aaron.brighton@deakin.edu.au
Figures 3, 8, 9, 12, 14 and 17–19 appear in color online: http://jcm.sagepub.com

0021-9983/09/20 2183–18 $10.00/0 DOI: 10.1177/0021998309344646

Recently, automotive manufacturers have been under increasing legislative pressure to reduce fuel consumption [3]. Reducing vehicle weight has a number of follow on benefits. If a weight reduction is realized in one area of a vehicle the effect of this cascades through the entire vehicle; engines, smaller brakes and power assistance systems as noted by Brosius [4]. Lower mass also reduces fuel consumption, not only reducing the cost to the consumer but also decreasing environmental impact. Additionally, in a collision the vehicle would have less momentum and therefore less energy needs to be dissipated to bring the vehicle to a stop.

Axial crushing of sample tubes has been shown to be representative of the behavior of crash structures in frontal impacts [5]. By definition, the area under a load-displacement curve is the energy absorbed during an event, with a rectangular load-displacement curve representing the maximum energy absorption capability of a material. The progressive crushing of fibre-reinforced plastic tubes approaches this ideal [6] (Figure 1).

To initiate the progressive crushing failure mechanisms some form of stress concentration is required to reduce the chance of catastrophic failure and reduce initial peak loads (Figure 1). Limiting these initial peak loads can minimize the possibility of the vehicle occupants experiencing forces above the threshold for human tolerance. The stress concentration or initiator, usually in the form a chamfer, is machined into one end of the tube. Another method used is the plug initiator with a varying radius to control the failure of composite tubes. This plug is a machined die, inserted into the end of the tube that becomes the crushing surface. Altering the radius of this plug produces varying results; as the radius approaches the wall thickness of the specimen the specific energy absorption (SEA) values increase [7].

Despite the obvious benefits of composites in energy absorbing structures the uptake of composite components by the automotive industry has generally been slow [8]. The development of the Quickstep 'out of autoclave' manufacturing process enables rapid manufacture of composite components without incurring excessive plant costs [9]. The Quickstep process utilizes the high heat transfer characteristics of Polyethylene Glycol

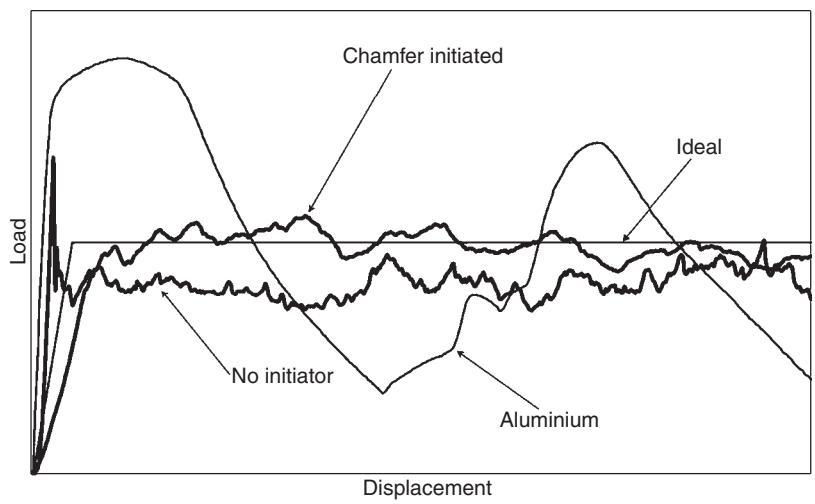

Figure 1. *Graph showing the typical response of metallic tubes, composite tubes with and without an 'initiator' and an idealized load line.*

(PEG), as opposed to the nitrogen gas commonly used in autoclaves. Due to the higher heat transfer rate of the liquid, shorter cycle times are achievable. The process does not require the use of high pressures; consequently less rigid, lower cost tooling is required. Both the aforementioned benefits of the Quickstep process aid in reducing the cost of the end product by increasing productivity and reducing capital costs.

METHOD

Test Specimens

Cylindrical test specimens with an outside diameter of 64 mm and nominal wall thickness of 2 mm (Figure 2) were manufactured using a male aluminium mandrel. The hollow aluminium mandrel had cam-lock connectors for the fluid inlet and outlet at one end (Figure 3). These connectors allowed the mandrel to be connected to the fluid lines of the Quickstep machine. The flowing fluid controls the temperature of the tool; as the tool heats up the aluminium expands and applies pressure to the part which aids with consolidation. As the tool cools it contracts to aid in part removal.

Carbon/Epoxy specimen tubes were manufactured using Toray G83C 12 K 2×2 twill 380 gsm as supplied by Toray Composites Tacoma, Washington USA (Table 1). The layup schedule was $[0/90]_4$ on the aluminium mandrel from a continuous roll of fabric. The 1 m length of Carbon/Epoxy tubing was then shrink-wrapped with 19 mm wide nylon shrink tape. A 4 mm shrink-wrap overlap was created using the tool feed feature using a tool shop lathe. The shrink-wrapped mandrel was then placed in a vacuum bag and connected to the Quickstep machine. The curing cycle employed a fast ramp to 100°C, dwelled for 5 min then a second fast ramp to 150°C and dwelled for 3 min. The mandrel was then brought

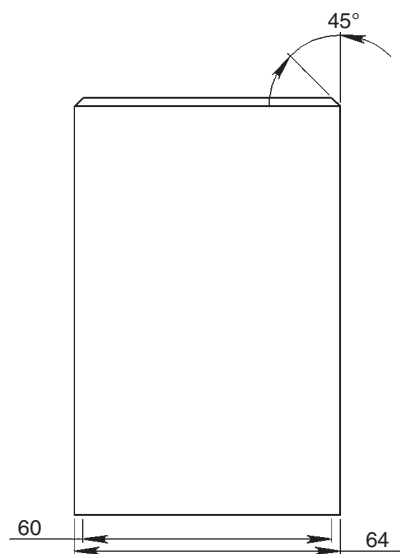

Figure 2. *General dimensions of tube specimens.*

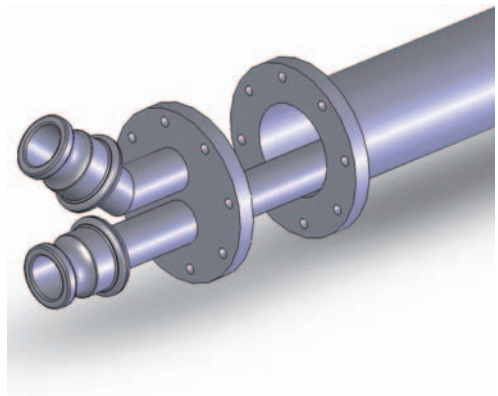

Figure 3. *Tube tool showing cam-lock connectors.*

Table 1. Properties of Toray G83C pre-preg and Twintex plain-weave fabric.

Toray G83C[5]			Twintex [18]		
Test type	**Property**	**Value**	**Test type**	**Property**	**Value**
In-plane tension	E_{11t}	52.2 GPa	In-plane tension	E_{11t}	13.79 GPa
	ν_{12}	0.028		ν_{12}	0.08
	σ_{ult}	1.037 GPa		σ_{ult}	287 MPa
	ε_{ult}	1.98%		ε_{ult}	3.3%
In-plane compression	$E_{11c}=E_{22c}$	55.4 GPa	In-plane compression	E_{11c}	5.3 GPa
	σ_{ult}	560 MPa		σ_{ult}	178 MPa
	ε_{ult}	1.01%		ε_{ult}	1.1%

down to a handling temperature of ~60°C; on average this took 3 min. This cure cycle took ~15 min in total.

The Twintex material (obtained from Saint-Gobain Vetrotex, France) consisted of a plain weave of commingled E-Glass/Polypropylene fabric (Table 1). Specimen tubes consisted of 4-layers held in place with a small amount of 3 M super 77 tack spray that were shrink-wrapped using the same method as used for the carbon tubes. The mandrel was then wrapped with 2 layers of 0.05 mm stainless steel and wool insulating material. The stainless steel was used as a heat reflector because the glass fibres acted as insulation preventing heat transfer to the outer layers. The cure cycle used was a fast ramp to 180°C, held for 1 min, before the mandrel was cooled to a handling temp of ~60°C, again on average this took 3 min. This cycle took ~20 min in total.

The tubes for dynamic testing were removed from the tool and each parent tube cut, using a diamond saw, into 250 mm specimens and labeled according to material type, parent tube and section from where the specimen was cut. The tubes for quasi-static testing were cut into 110 mm specimens and labeled.

These specimens were placed on a steel center in a lathe allowing one end to be square cut and the other to have a 45° chamfer cut. After machining, dynamic specimens had a nominal length of 240 mm and quasi-static specimens had a nominal length of 100 mm.

Figure 4. *Showing a plug initiator (left) and flat platen (right), both specimens have a 45 Chamafer.*

Testing Methodologies

Quasi-Static tests were performed on an MTS 100 kN screw driven load frame. Five forms of initiation were used for testing: 45° chamfer, 10 mm plug, 7.5 mm plug, 5 mm plug and 2.5 mm plug. Each initiator type was used with three specimens of Twintex tubes at a rate of 10 mm/min (1.67×10^{-4} m/s) between universal MTS compression platens. This approach was previously used by Silcock [10].

The dynamic tests were performed using a unique purpose built servo-hydraulic test machine built by MTS. Two forms of failure initiation were used, namely the 45° chamfer and the 45° chamfer combined with a 2.5 mm plug initiator (Figure 4). Each initiator type was utilized with both materials at speeds of 0.25, 0.5, 0.75, 1, 2, and 4 m/s. Each of these configurations used three specimens. Ram position, time, load cell (strain gauge load device), and load washer (piezoelectric load device) data were recorded at 4 kHz for the 0.25 m/s tests, 10 kHz for the 0.5 m/s tests and 20 kHz for the 0.75, 1, 2, and 4 m/s tests.

Utilizing the data the SEA was calculated for each test specimen per Equation (2) and average SEA values were reported for each test configuration.

$$\text{SEA} = \frac{\text{Energy Absorbed (kJ)}}{\text{Mass of Crushed Tube (kg)}} = \frac{\int_0^{x_f} \text{Load}\, \mathrm{d}x}{\text{Mass of Crushed Tube}} \tag{1}$$

$$\approx \frac{\text{Average Sustained Crush Load} \times \text{Crush Distance}}{\text{Mass of Crushed Tube}} \tag{2}$$

In addition to numerical data, each test was recorded using high-speed digital photography so failure modes and possible anomalies could be observed. When a large variance was evident in the results the high-speed video was consulted to look for potential testing abnormalities. Results from intermediate testing of Carbon/Epoxy tubes (Table 2) and Twintex tubes (Table 3) can be found in Appendix 1.

RESULTS AND DISCUSSION

Tube Crush Mechanisms

CARBON/EPOXY TUBES

The results from the quasi-static tests [10] showed that the 45° chamfer and the 2.5 mm plug produced the highest SEA values. Therefore, these initiators were selected for use during the intermediate rate tests. The trend for varying plug radii is shown in Figure 5.

Table 2. Results from intermediate speed testing of carbon/epoxy tubes.

Specimen	Test speed (m/s)	Initiator type	Peak load (kN)	Average crushing load (kN)	Crush distance (mm)	Specimen mass (g)	Specific energy (kJ/kg)	Load uniformity (%)
DT1-1	2	P	41.99	29.03	156.03	120.85	57.64	69.12
DT1-2	0.25	P	43.70	35.70	176.37	120.53	71.08	81.69
DT1-3	0.25	C	56.88	40.38	200.29	120.33	80.54	70.99
DT2-1	0.75	P	41.75	30.19	181.49	118.61	61.09	72.31
DT2-2	0.75	C	61.77	36.36	31.27	118.09	73.90	58.87
DT2-3	4	P	42.48	27.46	152.61	118.23	55.75	64.65
DT3-1	1	C	67.63	40.12	197.39	119.47	80.60	59.33
DT3-2	0.25	C	56.15	40.30	199.61	119.37	81.03	71.77
DT3-3	0.25	P	42.48	34.08	179.44	119.68	68.33	80.21
DT4-1	0.5	P	48.58	31.75	181.32	119.29	63.88	65.36
DT4-2	1	C	53.22	39.48	195.85	119.47	79.30	74.18
DT4-3	0.5	P	44.43	31.52	180.98	119.74	63.18	70.94
DT5-1	0.25	P	47.36	36.84	182.18	119.38	74.06	77.78
DT5-2	1	P	49.07	30.71	180.13	119.17	61.86	62.59
DT5-3	2	C	71.04	37.33	171.75	119.66	74.88	52.55
DT6-1	0.75	C	64.21	35.50	197.73	119.30	71.41	55.28
DT6-2	4	C	87.65	37.44	173.46	119.13	75.43	42.72
DT6-3	1	C	69.09	39.35	196.88	119.27	79.19	56.95
DT7-1	0.5	C	53.47	38.71	6.15	120.29	77.23	72.40
DT7-2	0.75	P	44.19	31.37	12.65	120.49	62.48	70.99
DT7-3	0.5	C	50.05	37.97	173.63	120.15	75.84	75.86
DT8-1	2	P	40.77	27.29	152.44	120.15	54.52	66.94
DT8-2	0.75	C	61.77	35.89	199.10	120.23	71.64	58.10
DT8-3	0.5	P	44.92	27.74	180.81	120.41	55.29	61.76
DT8-4	4	C	82.52	38.06	173.12	120.17	76.01	46.12
DT9-1	0.25	C	57.86	41.39	198.58	119.76	82.94	71.53
DT9-2	4	P	39.55	28.48	153.98	119.22	57.34	72.02
DT9-3	0.5	C	50.05	37.75	173.12	120.04	75.47	75.42
DT9-4	1	P	42.97	33.23	179.61	119.87	66.53	77.33
DT10-1	4	C	77.39	37.06	174.83	119.56	74.39	47.89
DT10-2	2	P	41.99	27.14	152.10	119.78	54.38	64.63
DT10-3	1	P	42.48	31.59	180.13	119.83	63.26	74.36
DT10-4	2	C	71.29	37.40	172.61	119.97	74.83	52.47
DT11-1	2	C	75.68	35.39	171.24	116.92	72.64	46.76
DT11-2	4	P	40.28	27.12	150.39	116.75	55.76	67.33
DT11-3	0.75	P	42.72	29.99	179.61	117.22	61.40	70.19

Energy absorbed during axial crush tests is dependent upon the failure modes that develop during the crush. Composite tubes usually fail in one of three ways [11]:

(1) Catastrophic collapse (Euler buckling),
(2) Shell buckling, leading to hinge formation, and progressive folding and
(3) Brittle fracture

The Carbon/Epoxy tubes in this study failed by brittle fracture. The fractured material from the pre damaged (chamfered) edge forms a debris wedge that initiates a mode I interlaminar fracture (Figure 6) up the mid wall of the tube. When this material is forced out, axial tears develop to allow for the circumferential expansion. As these axial tears propagate up the tube the hoop fibres are stressed until failure allowing the crack to

Table 3. Results from intermediate speed testing of Twintex tubes.

Specimen	Test speed (m/s)	Initiator type	Peak load (kN)	Average crushing load (kN)	Crush distance (mm)	Specimen mass (g)	Specific energy (kJ/kg)	Load uniformity (%)
DTT1-1	1	P	35.40	27.68	181.84	143.70	46.61	78.19
DTT1-2	4	C	73.58	29.25	200.15	143.83	49.22	39.75
DTT2-1	0.25	P	36.62	28.57	182.69	142.97	48.35	78.00
DTT2A-3	1	P	36.13	28.58	178.59	143.21	48.29	79.09
DTT2-3	0.75	P	39.55	27.60	180.47	143.12	46.67	69.79
DTT3-1	0.75	C	37.84	19.96	199.61	143.58	33.64	52.74
DTT3-2	0.75	P	35.64	25.13	180.98	143.80	42.30	70.51
DTT3-3	2	C	40.04	28.50	171.41	143.42	48.09	71.18
DTT4-1	2	C	41.26	30.60	171.58	143.21	51.71	74.17
DTT4-2	1	P	34.91	25.27	181.32	142.54	42.91	72.39
DTT5-1	0.75	C	42.72	22.31	199.27	142.55	37.87	52.22
DTT5-2	2	P	34.91	23.29	154.49	142.89	39.44	66.71
DTT6-1	4	P	32.47	19.03	151.42	143.54	32.08	58.61
DTT6-2	4	C	38.57	22.63	172.95	142.78	38.36	58.67
DTT6-3	2	C	35.16	18.94	171.75	142.88	32.08	53.87
DTT7-1	0.5	C	24.41	15.23	173.12	132.38	27.85	62.40
DTT7-2	1	C	31.25	16.74	199.78	132.78	30.52	53.58
DTT7-3	4	P	32.47	19.17	155.52	132.55	34.99	59.03
DTT8-1	4	C	46.63	28.73	168.85	143.02	48.61	61.60
DTT8-2	0.5	C	39.31	20.53	202.69	142.97	34.75	52.24
DTT8-3	1	C	32.47	20.00	199.78	142.77	33.91	61.61
DTT9-1	1	C	43.21	25.72	199.95	141.49	43.99	59.51
DTT9-2	0.75	C	39.31	25.17	198.75	141.49	43.05	64.04
DTT10-1	0.25	C	36.38	24.75	200.98	143.54	41.73	68.04
DTT10-2	0.25	P	33.20	21.06	182.18	143.24	35.58	63.42
DTT10-3	2	P	34.67	24.77	152.78	142.65	42.02	71.44
DTT10-4	0.75	P	40.53	28.21	180.30	142.97	47.76	69.62
DTT11-1	0.25	C	40.53	32.58	198.75	143.00	55.14	80.39
DTT11-2	4	P	40.77	25.56	154.83	142.61	43.37	62.68
DTT11-3	0.25	P	34.67	24.98	182.35	142.71	42.36	72.06
DTT12-1	0.5	P	35.64	26.20	181.67	142.88	44.38	73.51
DTT12-2	0.5	C	41.50	30.33	200.98	142.65	51.46	73.08
DTT12-3	0.5	P	34.42	24.98	180.47	142.92	42.30	72.57
DTT13-1	0.5	P	40.77	29.81	181.49	143.25	50.36	73.12
DTT13-2	0.25	C	42.72	35.53	202.34	143.33	59.99	83.17
DTT13-3	2	P	37.84	29.11	149.71	143.31	49.16	76.92

propagate further. The axial tears result in fronds that deform as they are forced through the failure zone (Figure 7).

It has been suggested by Fairfull and Hull [12] that as much as 50% of the energy absorbed during tube crushing can be attributed to various frictional processes. These frictional processes include [12] (Figure 6):

(1) Laminar bundles sliding against the crushing surface (platen),
(2) Laminar bundles sliding relative to one another, and
(3) Adjacent material sliding against the debris wedge

A significant difference was observed in both the energy absorbed and the failure mechanism of the 2.5 mm plug initiated specimens and the 45° chamfer-initiated specimens.

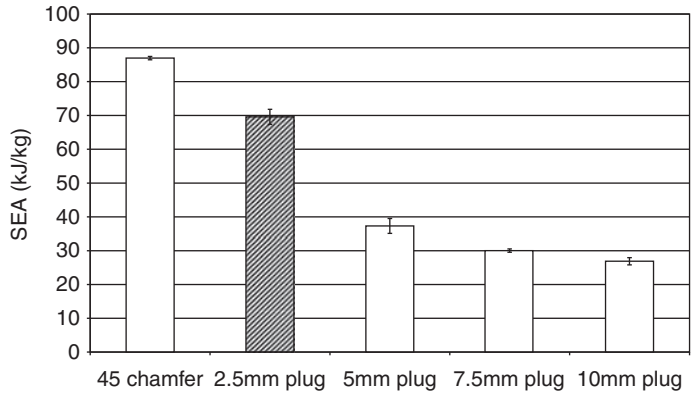

Figure 5. *Carbon tube performance for different forms of initiation at quasi-static rates from Silcock [10]. Hatched data represents data added by the author.*

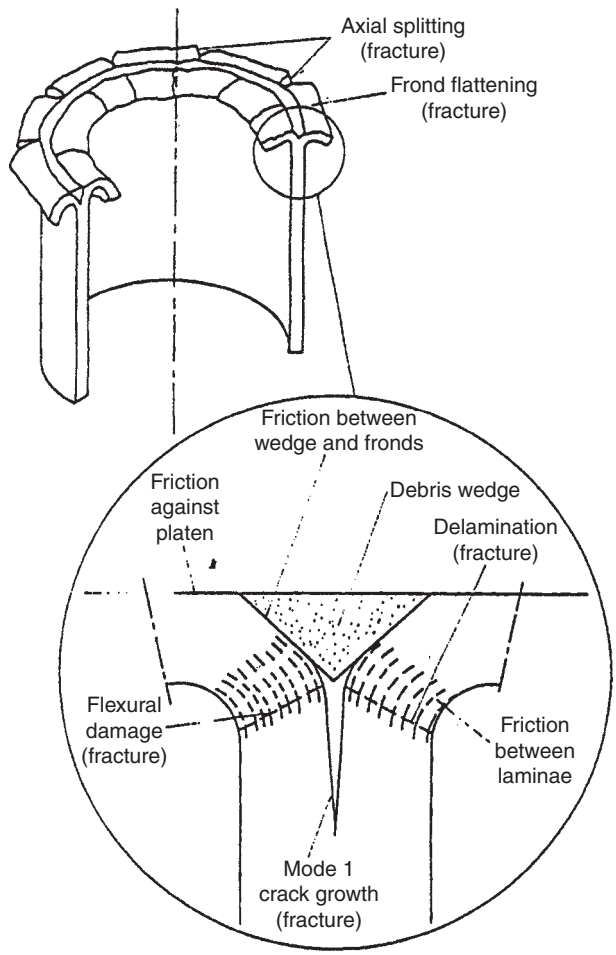

Figure 6. *Sources of energy absorption in the crush zone [12].*

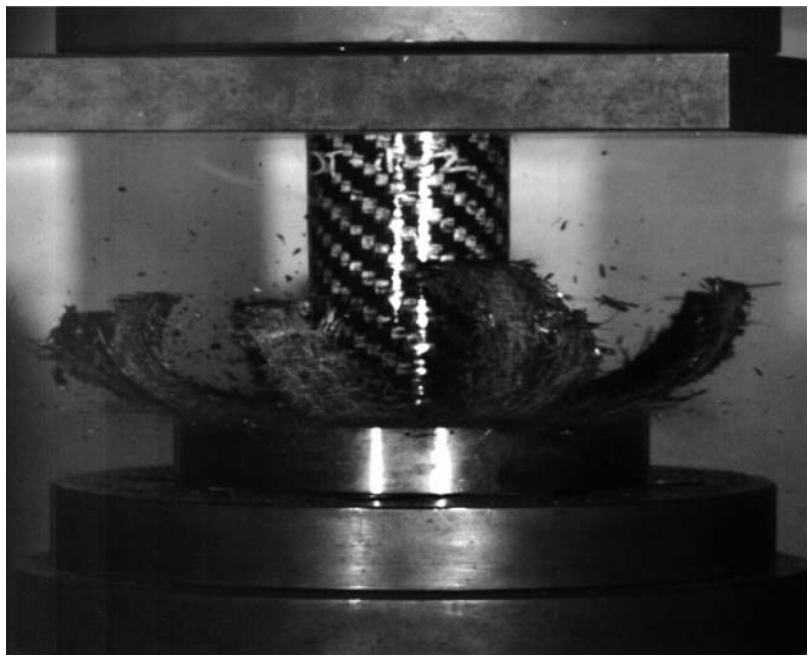

Figure 7. *Frond development during 2.5 mm plug initiated test at 4 m/s of carbon/epoxy.*

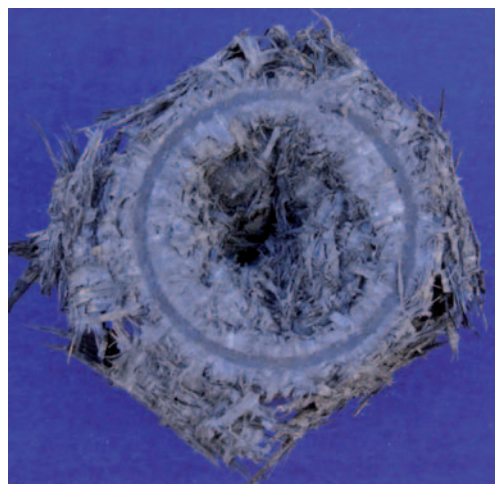

Figure 8. *The debris wedge and failed material in the center of the tube formed during 45 chamfer tests of carbon/epoxy.*

During the 2.5 mm plug tests all fibres splayed outwards; the only failure evident was the breakage of hoop fibres as the plug forced the laminate out and the axial tears propagated up the tube. In addition to hoop fibre failure, frictional effects 1 and 2 as defined previously added to the energy absorbed.

By contrast during the 45° chamfer initiated tests, some of the failed material formed a debris wedge (Figures 8 and 9). This debris wedge caused a mode I interlaminar failure [12]

at mid thickness which resulted in approximately half of the material to be forced into the center of the tube (Figure 6). The formation of this debris wedge is responsible for the inclusion of both a mode I failure mechanism and the addition of the third frictional process described above and shown in Figure 6. It is the addition of these processes that explains the higher SEA of the 45° chamfer initiated specimens over the 2.5 mm plug initiated specimens. Typical force displacement curves from tests conducted using both the 45° chamfer and 2.5 mm plug initiator can be seen in Figure 10.

Figure 9. *Fracture zone showing failed material and debris wedge in Carbon/Epoxy specimen.*

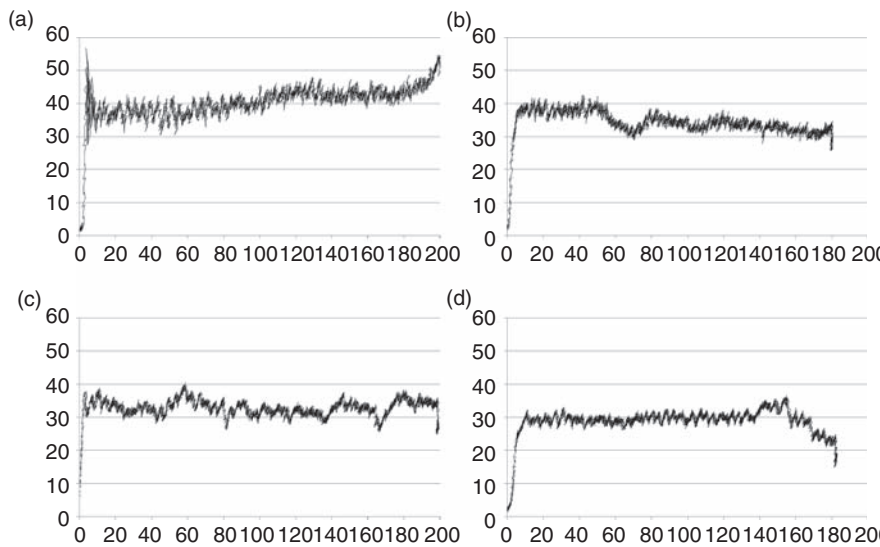

Figure 10. *Graphs showing typical force (kN) displacement (mm) curves during axial compression testing: (a) Carbon specimen at 0.25 m/s using a chamfer initiator, (b) Carbon specimen at 0.25 m/s using a plug initiator, (c) Twintex specimen at 0.25 m/s using a chamfer initiator, (d) Twintex sample at 0.25 m/s using a plug initiator.*

It should also be noted that after the 45° chamfer initiated tests were complete and the cross head had returned, the specimen had adhered to the platen. A possible explanation for this could be that enough heat was generated by friction in the crush zone to cause the resin to pass its T_g. This rise in temperature may have caused any uncured resin to react and bond the specimen to the crushing surface.

GLASS/POLYPROPYLENE TUBES

Quasi-static testing of the Glass/Polypropylene tubes produced a similar trend to the carbon. As the radius of plug initiator approached the wall thickness of the specimen, the energy absorbed increased (Figure 11).

During the quasi-static tests it was observed that the Glass/Polypropylene tubes failed by progressively folding in a combination of concertina and diamond folding. This folding was similar to that observed in the axial crushing of steel and aluminium tubes (Figure 12). When the test speed was increased the Twintex tubes underwent external inversion (Figure 13). This inversion takes place when the material at the fracture zone folds back on itself. As the crush progresses the tube effectively turns inside out. When the failed material comes into contact with the platen it concertinas to allow more material to invert.

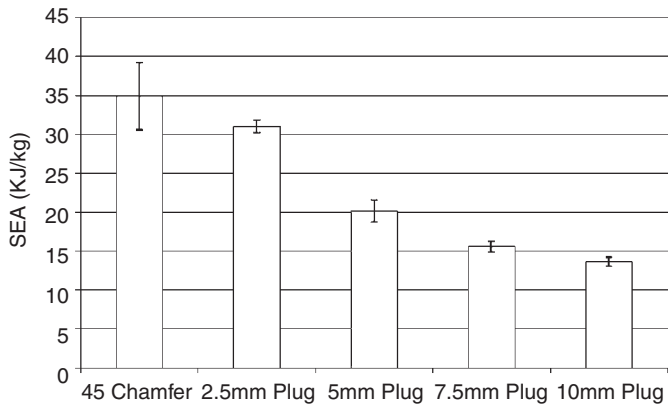

Figure 11. *SEA values of Twintex material using different forms of initiation at quasi-static rates showing an increase as the radius of the plug initiator is decreased.*

Figure 12. *Concertina and diamond crush modes as seen in metallic tubes (left and center) [5] and Twintex tubes (right).*

A similar failure mode was experienced during testing of a hybrid CF/AF-EP crash element for the Audi A8 [13]. Force-displacement curves for both chamfer initiated and plug initiated specimens can be seen in Figure 10.

High-speed photography of specimen crushing revealed that the failure modes experienced using both the 45° chamfer and the 2.5 mm plug appeared to be similar. However, the inversion process when using the 2.5 mm plug was more repeatable. While the same behavior was observed in the 45° chamfer-initiated tests it took between a quarter and a half of the test before this failure mode appeared.

Inspection of the post crush 45° chamfer initiated specimen revealed building of debris in the center of the tube (Figure 14). The debris appeared to have acted in a similar manner as a plug initiator and thus shall be referred to as a 'debris plug'. This debris plug forced the remainder of the tube to undergo the inversion process in a similar manner as the plug initiated specimens. However, this debris plug did not reliably form and the inversion was not nearly as uniform around the circumference as with the machined plug initiator.

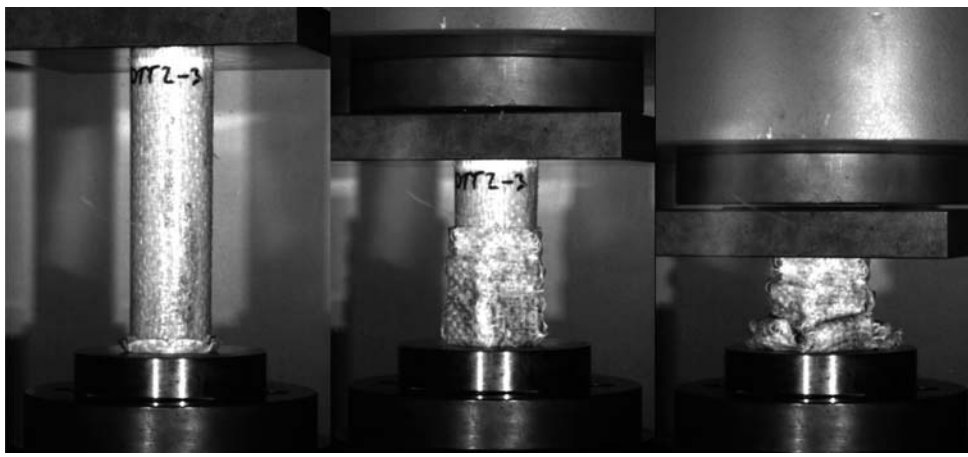

Figure 13. *Twintex tube undergoing inversion during plug-initiated test at 4 m/s.*

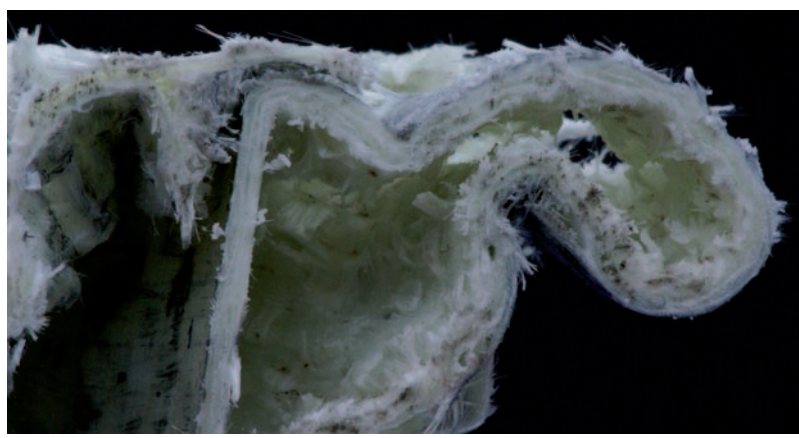

Figure 14. *Debris plug and material inversion of Twintex tube during 45° chamfer initiated test.*

The ductility of the thermoplastic matrix is more prone to plastic deformation as opposed to the brittle fracture evident in a thermoset matrix. Due to this and its higher toughness, small debris fragments do not form the wedge as seen in the Carbon/Epoxy specimens. Also due to the toughness of the matrix the material resists mode I crack formation, instead the debris plug, as discussed above, forms. Due to the lack of this debris wedge and the resulting mode I fracture the third friction process did not occur. This is believed to have contributed to the lower SEA when compared to the carbon specimens.

STRAIN RATE BEHAVIOR

Carbon/Epoxy Tubes

During 45° chamfer testing it was found that there was a 15% drop in load across testing speeds (Figure 15). The highest variability was 3 kJ/kg or 3.4% during the 0.75 m/s test. With the exception of the 0.5 m/s test the trend is negative. That is, as test speed increases the SEA drops. This correlates with work conducted by Ramakrishna [14] and Thornton [15], however, it conflicts with data presented by Farley [16] in which an increase in energy absorption was seen.

It was also seen that 2.5 mm plug tests showed a 22% drop in load across the testing speeds. However, there was a larger variability present with 12 kJ/kg or 16.9% occurring during the 0.5 m/s tests (Figure 16).

As the speed of the 2.5 mm plug tests was increased from 0.5 to 4 m/s, the behavior of the fronds was seen to change. During the 0.5 m/s tests the fronds were found to have a tight radius of curvature (Figure 17), however, at higher crush rates the radius of curvature increased (Figure 18) until the 4 m/s test in which the fronds were not observed to curl much at all (Figure 19).

The radius of curvature of the fronds developed during 2.5 mm plug initiated tests (Figures 17–19) can possibly explain the drop in load as test speed increases. The smaller the radius of curvature of the developing fronds, seen in the 0.5 m/s test, resulted in a larger

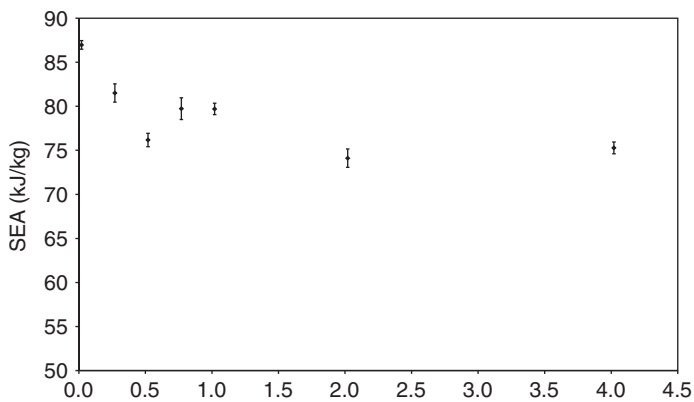

Figure 15. *SEA vs test speed (m/s) for carbon tubes using a 45° chamfer.*

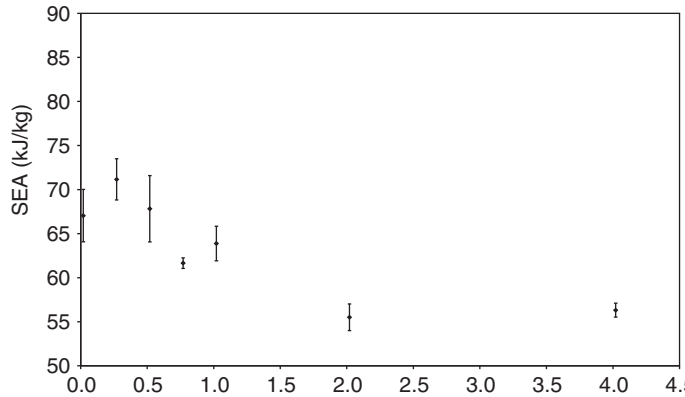

Figure 16. *SEA vs test speed (m/s) for carbon tubes using a 2.5 mm plug initiator.*

Figure 17. *Tight fronds developed in Carbon/Epoxy specimen at 0.5 m/s impact speeds.*

Figure 18. *Separated fronds developed in Carbon/Epoxy specimen at 2 m/s impact speed.*

Figure 19. *Unwound fronds developed in Carbon/Epoxy specimen at 4 m/s impact speed.*

number of cracks at the failure zone; this translates into higher SEA values as more damage is done to the material. Conversely, the increasing radius of curvature seen in the 2 and 4 m/s test resulted in a lower number of cracks, hence less energy absorbed (Figure 20).

Glass/Polypropylene Tubes

Different testing speeds used with the Twintex tubes resulted in a large range of SEA values. Twintex tests with the 45° chamfer resulted in a 39% variation between the highest and lowest values. This was attributed to the difference in failure modes as discussed earlier. At 0.25 m/s the inversion failure mode became evident, after this the average SEA values fell rapidly to 44 kJ/kg (Figure 21).

While using the 2.5 mm plug a 40% difference between the highest and lowest SEA was evident across the testing speeds (Figure 22). Using the 2.5 mm plug as an initiator the peak in SEA did not occur until the 0.5 m/s tests. The energy absorption capacity then dropped off as test speeds increased. However, there was a large amount of variation within each set of test conditions, some tests exhibited a relative error of up to 40%. Therefore, due to the scatter within each test set-up this trend cannot be stated with any certainty.

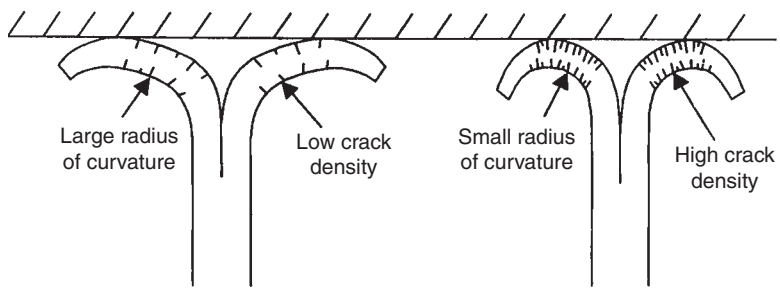

Figure 20. *Crack density vs radius of curvature [7].*

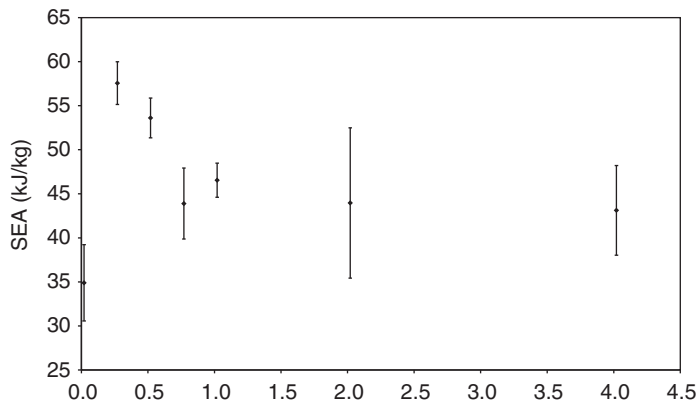

Figure 21. *SEA vs test speed (m/s) for glass/polypropylene tubes using a 45° chamfer.*

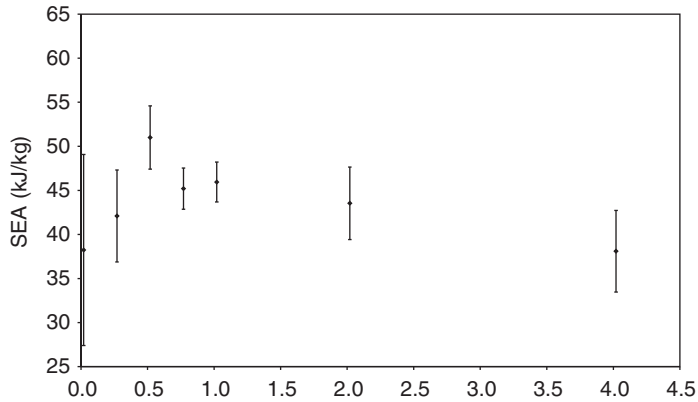

Figure 22. *SEA vs test speed (m/s) for glass/polypropylene tubes using a 2.5 mm plug.*

Due to the nature of this material i.e., dry fibre pre-preg, it was difficult to ensure fibre alignment along the full length of the tube and through all layers. The dry fibre had no tack, therefore took a lot more effort to ensure a tight wrap to reduce the likelihood of wrinkles occurring. Also due to the instability of the weave the fibres at the edges were prone to fraying no matter how carefully the material was laid on to the mandrel. These factors may have contributed to the wide spread of data within each test configuration.

A limitation of the Quickstep system is the difficulty in accurately controlling the cooling rate. This generally resulted in a range of cooling rates between 18 and 25°C/min for the Twintex tubes manufactured. However, one tube experienced a cooling rate of 38°C/min. This tube yielded two specimens, both of which did not exhibit any statistical anomalies. By comparison to results from Wasiak et al. [17], it can be seen that these rapid cooling rates would not have allowed high degrees of crystallinity formation.

It should be noted that Wasiak's work was conducted on isotactic polypropylene without glass reinforcement. The absence of the glass fibres reduces the nucleation surfaces. Further research is required in this area to quantify the degree of crystallinity of the specimens and the effect of cooling rate and crystallinity on the SEA and failure modes.

CONCLUSION

Carbon/Epoxy and Glass/Polypropylene tubes were crushed at speeds ranging from 1.67×10^{-4} m/s to 4 m/s to determine the energy absorption capability. Quasi-static testing showed that the 45° chamfer and 2.5 mm plug initiator produced the highest SEA values. It was found that as testing speed increased, SEA values for Carbon/Epoxy tubes decreased for both the 45° chamfer and 2.5 mm plug initiated tests. These tubes exhibited up to a 22% decrease in energy absorption capability.

Impact tests involving the Twintex tubes were not found to reach their peak SEA values until speeds of 0.25 m/s for the 45° chamfer and 0.5 m/s for the 2.5 mm plug initiated tests. Once the inversion failure mechanism developed, the energy absorption dropped by up to 40% across the test speed range. However, due to a large spread of data within each test configuration this trend cannot be stated with much certainty.

Both matrix systems had a strain rate response although the polypropylene matrix showed a greater dependence on impacting speed but with a higher degree of uncertainty. While the Carbon/Epoxy tubes exhibited the same failure mechanisms through all speeds, the failure mode of the Twintex tubes varied with speed. The most obvious change was noted between the quasi-static tests in which a ductile folding failure was seen and the intermediate test in which a more brittle fracture was observed. The 45° chamfer Carbon/Epoxy tests showed the highest SEA and the least dependence on speed. This group of tests also showed the smallest relative error.

ACKNOWLEDGMENTS

The author would like to thank the Victorian Centre for Materials and Manufacturing (VCAMM) for the financial support of this work, Oak Ridge National Laboratories for the use of Facilities and Peter Brighton for the still photography.

Research sponsored by the Assistant Secretary for Energy Efficiency and Renewable Energy, Office of Freedom CAR and Vehicle Technologies, as part of the Automotive Lightweighting Materials Program and the High Temperature Materials Laboratory User Program, Oak Ridge National Laboratory, managed by UT-Battelle, LLC, for the U.S. Department of Energy under contract number DE-AC05-00OR22725. This document was prepared by Quickstep technologies as a result of the use of facilities of the U.S. Department of Energy (DOE) that are managed by UT-BATTELLE, LLC. Neither UT-BATTELLE, LLC, DOE, or the U. S. government, nor any person acting on their behalf: (a) makes any warranty or representation, express or implied, with respect to the information contained in this document; or (b) assumes any liabilities with respect to the use of, or damages resulting from the use of, any information contained in the document.

REFERENCES

1. Dreyfus, M.K. and Viscusi, W.K. (1995). Rates of Time Preference and Consumer Valuations of Automobile Saftey and Fuel Consumption, *Journal of Law and Economics*, **38**(1): 79–105.
2. Fowler, D. (2004). A Crashworthy Diet, *The Engineer Magazine*, 6–19 February, pp. 24–29.
3. Jambor, A. and Beyer, M. (1997). New Cars-new Materials, *Materials and Design*, **18**(4–6): 203–209.
4. Brosius, D. (2003). Carbon Fiber Gains Traction with Automakers, *Dale Brosius, Composites Technology*, August: 32.
5. Silcock, M.D. (2007). *Composite Crashworthy Structures Manufacturing and Modelling, CMFI*, Deakin University, Geelong.
6. Carruthers, J., Kettle, A.P. and Robinson, A.M. (1988). Energy Absorption Capability and Crashworthiness of Composite Material Structures: A Review, *Applied Mechanical Review*, **51**(10): 635–649.
7. Fernie, R. (2002). Loading Rate Effects on the Energy Absorption of Lightweight Tubular Crash Structures, *School of Mechanical, Material, Manufacturing Engineering and Management*, University of Nottingham, Nottingham.
8. Knight, H. (2003). Weighing up the Advantages, *The Engineer Magazine*, 5–18 December, pp. 8–9.
9. Bader, M.G. and Noble, N. (2004). A Comparison of the Costs of Manufacture of a Laminated Composite Component by Conventional Autoclave and a Novel Non-autoclave Process, *25th Jubilee International SAMPE Europe Conference*, Porte de Versailles, Paris.

10. Silcock, M.D. (2006). Raw Data from Quasi-static Testing of Carbon Tubes during Initiator Optimisation Study, In: Brighton, A. and Geelong, P. (eds), *CSV Files Containing Raw Data from Testing*, Unpublished, Deakin University.
11. Hull, D. (1991). A Unified Approach to Progressive Crushing of Fibre-reinforced Composite Tubes, *Composites Science and Technology*, **40**: 377–421.
12. Fairfull, A.H. and Hull, D. (1988). Energy Absorption of Polymer Matrix Composite Structures – Frictional Effects, *Structural Failure*, 255–279.
13. Dyckhoff, J. and Haldenwanger, H.-G. (2003). Fibre-reinforced Composite Plastic Side Member with Crash Compatibility, *Business Briefing, Global Automotive Manufacturing & Technology*.
14. Ramakrishna, S. and Hull, D. (1993). Energy Absorption Capability of Epoxy Composite Tubes with Knitted Carbon Fibre Fabric Reinforcement, *Composites Science and Technology*, **49**: 349–356.
15. Thornton, P.H. and Edwards, P.J. (1982). Energy Absorption in Composite Tubes, *Journal of Composite Materials*, **16 November**: 521–545.
16. Farley, G.L. (1991). The Effects of Crushing Speed on the Energy-absorption Capability of Composite Tubes, *Journal of Composite Materials*, **35**: 1314–1329.
17. Wasiak, A., Sajkiewicz, P. and Wozniak, A. (1999). Effects of Cooling Rate on Crystallinity of I-Polypropylene and Polyethylene Terephthalate Crystallised in Nonisothermal Conditions, *Journal Of Polymer Science: Part B Polymer Physics*, **37**: 2821–2827.
18. Brown, K., Brooks, R. and Warrior, N. Numerical Simulation of Damage in Thermoplastic Composite Materials, In: *5th European LS-DYNA Users Conference*, Birmingham, UK.